J|A|C|S
COMMUNICATIONS

Published on Web 10/24/2006

Direction Specific Interactions of 1,4-Dicarboxylic Acid with Calcite Surfaces

H. Henry Teng,*,† Yang Chen,‡ and Elli Pauli†

Department of Chemistry, George Washington University, Washington, D.C. 20052, and Department of Earth Sciences, Nanjing University, Nanjing, Jiangsu 210093

Received May 5, 2006; E-mail: hteng@gwu.edu

Calcite is the most abundant biogenic carbonate and represents the largest carbon reservoir in the earth system. Interaction of carboxylic acids (CA) with carbonate minerals is a key component of many natural processes. In geological settings, the acids affect the dissolution and precipitation[1] of minerals as well as the adsorption of solutes to mineral surfaces.[2] In biological systems, carboxyl groups in biomacromolecules play a critical part in directing the biomineralization of functional inorganic tissue components.[3] This interaction is expressed in chiral selection,[4,5] crystal size, morphology, and orientation preference,[6,7] and polymorph stabilization.[8]

Because of the similarity between the carbonate anion (CO_3^{2-}) and the carboxyl group ($-COO^-$) of carboxylic acids, the CA-calcite interaction is generally understood to result from the electrostatic attraction of the negatively charged aqueous $-COO^-$ and positively charged Ca surface sites.[4,7,9] This indicates that, given the anisotropy of crystal lattice, the interaction must be crystallographic direction specific. Although such understanding has led investigators to achieve oriented nucleation on fixed substrates,[6,10] the binding mechanism of free aqueous carboxylic acids on the surfaces of carbonate minerals remains to be elucidated. Our previous studies[4,7] of calcite−aspartic acid (ASP) interactions revealed the development of steps in several geologically uncommon directions on calcite $\{10\bar{1}4\}$ cleavage faces and suggested that these directions represented the preferred orientations for ASP to bind on calcite surfaces. Investigations using pure enantiomers of ASP documented a crystallographic symmetry breaking on growth hillocks and etch pits with reference to the existing reflective symmetry element, as well as the mirror relationship between the growth or dissolution features developed in the presence of D- and L-ASP, respectively.[4] These studies, meanwhile, left open questions regarding the involvement of ASP's functional groups and the geometry of the surface binding. For example, it is not clear whether the ASP molecules "lie" on the crystal face with both of their carboxyls binding to the steps or "stand" with only one of the carboxyls attached to a surface site. Unaddressed issues seem to focus on the roles of the ASP's side chain carboxyl and the α-amine in the surface binding.

An effective strategy to gain a deeper insight into the ASP−calcite interfacial reaction is to monitor the changes in the surface microtopography of calcite while systematically varying the functional groups and the side chain properties of ASP. This can be done by using various derivatives of ASP, such as serine (different functional group on the side chain) and glutamic acid (different side chain length). In this study, we used succinic acid (SUC) to react with calcite. SUC and ASP may be related through the following schematic elimination reaction (eq 1):

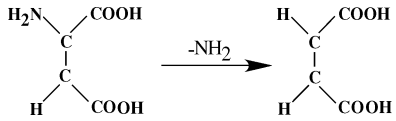

SUC shares the same carbon backbone of ASP but does not have an amine group. The loss of amine and, hence, the chirality on the α-C leaves SUC symmetrical. Results of the SUC-calcite reaction thus are expected to (a) implicate the involvement of the α-NH_2 group, or the lack thereof, in ASP's binding on calcite surfaces, and (b) confirm the necessity of chiral molecules in inducing crystallographic symmetry breaking on calcite $\{10\bar{1}4\}$ faces.

The calcite $\{10\bar{1}4\}$ cleavage faces were reacted with SUC solutions of different concentrations. Prior to injecting SUC, the substrate surface was first exposed to water in the reaction chamber to produce $\langle\bar{4}41\rangle$ rhombus etch pits which were used to establish the samples' crystallographic orientation. Upon the introduction of SUC into the H_2O-calcite system, accelerated dissolution by the acid induced a quick change in the roughness of mineral surfaces, usually within a few seconds (Figure 1A). As expected from the previous study,[7] in situ atomic force microscopy (AFM) revealed that the changes in the surface microtopography resulted primarily from the appearance of newly formed etch pits. At a SUC concentration of 1 mM, the pits maintained the well-defined rhombic morphology commonly observed in water and inorganic acids,[7,11] regardless of the solution pH. The pits began to take on a hexagonal shape when the SUC concentration increased to 10 mM at pH = 3 (Figure 1A,B). The six-sided pits also dominated initially when the SUC concentration was further increased to 100 mM. However, continuous reaction at this high SUC concentration led the pit morphology to evolve from six-sided to seven-sided (Figure 1C) and finally to five-sided (Figure 1D) irrespective of pH. A summary of experimental observations is given in Table 1.

Reflecting the rhombohedral symmetry ($R\bar{3}/2c$) of a calcite unit cell, the pits on the $\{10\bar{1}4\}$ faces developed in water are bounded by the $[\bar{4}41]$ and $[48\bar{1}]$ vectors[12] that are related by the only symmetry element, a *c*-glide plane, perpendicular to this surface. The two positive edges of the pits, $[\bar{4}41]_+$ and $[48\bar{1}]_+$, are crystallographically equivalent and so are the two negative ones, $[\bar{4}41]_-$ and $[48\bar{1}]_-$. It is evident that the $\langle\bar{4}41\rangle$ edges in water are the slowest moving ones because any steps that have higher rates of motion should literally grow themselves out of existence. Thermodynamically, this makes sense because the monolayer steps in these directions are composed of alternating Ca and CO_3 and are the most stable during calcite growth and dissolution in the absence of any additives.[13] An examination of the shapes of the 5-, 6-, and 7-sided pits indicates that these polygons differ from the common $\langle\bar{4}41\rangle$ rhombus by the presence of additional edges along the $[42\bar{1}]$ and/or [010] vectors (Figure 2A). The development of the hexagon requires a decreasing dissolution rate along the $[42\bar{1}]$ relative to all other directions. The morphological evolution from

† George Washington University.
‡ Nanjing University.

10.1021/ja063167m CCC: $33.50

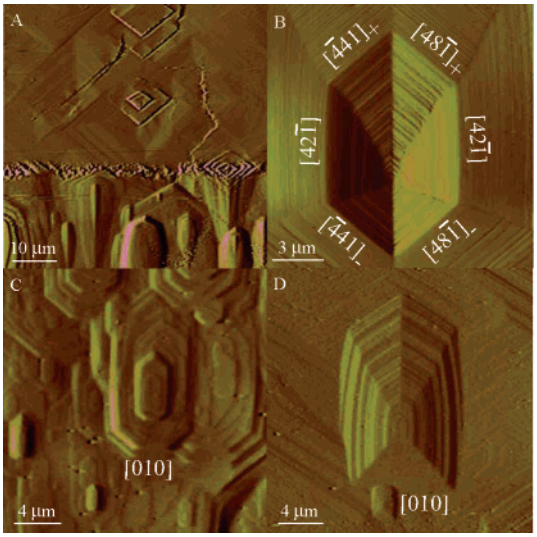

Figure 1. In situ deflection mode AFM images showing (A) the rapid (within 6 s) change of surface topography upon the input of SUC (blurred horizontal band), (B) the hexagonal, (C) the 7-sided, and (D) the 5-sided pits developed at different SUC concentrations. The rhombic morphology seen in water is shown in the upper half of panel A.

Table 1. Summary of observed changes in pit morphology

	SUC concentration (M)		
	<0.001	0.01	0.1
pH 3	rhombus	hexagon	6- → 7- → 5-sided
pH 5,6	rhombus	rhombus	6- → 7- → 5-sided

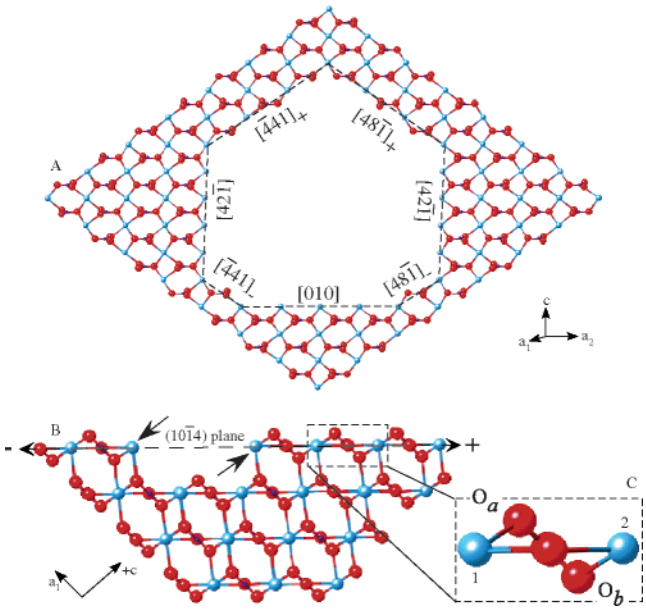

Figure 2. Crystal structure of calcite {10$\bar{1}$4} faces showing (A) the atomic arrangements of the step edges surrounding the etch pits developed in SUC; (B) profile view of a (10$\bar{1}$4) plane and a one-layer deep etch pit when viewed in the [010] direction; and (C) the positions of different oxygen atoms of the CO_3 groups relative to the (10$\bar{1}$4) surface, as well as the binding geometry of these oxygens with the in-plane Ca. Notice the relative (to the $+c$ direction) position of the Ca (1 and 2 in C) bound by the oxygens above (O_a) and below (O_b) the plane. The solid arrows in part B indicate the bond directions in which SUC approaches the pit edges.

the six-sided to the seven-sided and eventually to the five-sided on the other hand is a direct result of the gradually slowing rate of retreat of the [010] step relative to the [$\bar{4}41$] $_-$ and [48$\bar{1}$] $_-$ steps. This implies that SUC changes the relative speed of the ⟨$\bar{4}41$⟩, [42$\bar{1}$], and [010] steps in addition to facilitating the overall dissolution of calcite. Specifically, the presence of SUC decreases the values in the ratio of v[42$\bar{1}$]/v⟨$\bar{4}41$⟩ and v[010]/v⟨$\bar{4}41$⟩ where v is the step velocity. However, because [42$\bar{1}$] and [010] steps do not develop in water, we cannot know for certain if the decrease is due to an increase in v⟨$\bar{4}41$⟩, a decrease in v[42$\bar{1}$] and v[010], or both. It is also possible SUC enhances the speed in all directions, but the increase is more substantial for v⟨$\bar{4}41$⟩ than for the other two directions. Furthermore, in spite of the low stability of the [42$\bar{1}$] and [010] steps in water,[13] we do not have enough information to ascertain whether the change of relative step speed is due to thermodynamics (i.e., lower step energies for [42$\bar{1}$] and [010]) or kinetics (i.e., surface poison or impurity inhibition). This is largely because the system is far away from equilibrium (i.e., the saturation is not controlled in the experiments). Measurements of pit size indicate that both ⟨$\bar{4}41$⟩ and [42$\bar{1}$] edges retreat faster at higher SUC concentrations (0.01 vs 0.1 M). One of the implications of this observation is that, at these concentrations, more aqueous phase SUC does not translate into higher levels of adsorption on the surface or the ligand binding is saturated at the lower SUC concentration. On the other hand, pit morphology, and hence the development of new step directions, does show a dependence upon SUC concentration (see Table 1), suggesting that the surface coverage is still controlled by the amount of aqueous SUC and is critical for slowing down the new steps.

It is well-established that certain additives can alter the stability or kinetics of crystal faces during dissolution or crystallization.[14] The strong affinity of $-COO^-$ toward Ca^{2+} in aqueous media suggests that SUC, a dicarboxylic acid and hence a bidentate ligand, should bind strongly to terminal Ca on calcite crystal faces as well to alter the surface property. The well-defined anisotropy in the etch pits revealed by Figure 1 implies the existence of a robust interaction between SUC and calcite in the crystallographic directions developed therein. We propose that the observed changes in pit morphology result from a selective binding of SUC along certain specific directions. Three mechanisms may exist for SUC and calcite steps to recognize each other at a molecular level,[15] namely electrostatic matching, geometric correspondence, and stereochemical conformity. Viewing the molecular structure of SUC (eq 1), one finds that the only reactive sites are the 1- and 4-carboxyl groups. This indicates that an electrostatic matching is favored at steps where Ca atoms are contiguous. Whereas a (10$\bar{1}$4) plane contains an equal amount of Ca and CO_3, inspection of the atomic structure of the {10$\bar{1}$4} faces (Figure 2A) reveals that both the [42$\bar{1}$] and [010] satisfy this requirement. These two directions are not commonly seen in geological settings presumably owing to their fast growth or dissolution rates associated with the high step energies in the absence of additives.[13] Their development in SUC solutions suggests that a strong electrostatic interaction with a chelating ligand is able to slow the step motion either through enhancing the step stability or by inhibiting the dissolution kinetics.

Geometric correspondence can be checked by surveying the distance between carboxyls on SUC and that between adjacent calciums in the two directions. The Ca atoms in the [010] and [42$\bar{1}$] steps are separated by 4.05 and 4.99 Å, respectively. While these distances at step edges are largely fixed, the separation between the SUC carboxyls is variable because of the rotational flexibility of the C−C single bonds. For a coplanar configuration with reference to the four C atoms in SUC, when both carboxyls are on the same side of the C_2-C_3 bond (eq 1), one can show that, through the rotation of the C_1-C_2 and C_3-C_4 bonds, the minimal and maximal distance for the inter-carboxyl oxygen atoms is approximately 1.3 and 5.6 Å, respectively. Such a wide range makes

it possible for the $-COO^-$ groups to bind simultaneously with adjacent Ca atoms along either the [42$\bar{1}$] or [010] steps.

We noticed that the position of the [010] edge always lies in the negative end of the $\langle\bar{4}41\rangle$ rhombus. To understand the anisotropic appearance of the [010] steps, one needs to look into the possible stereochemical effect on the {10$\bar{1}$4} faces in addition to the charge and geometric recognition. It is important to point out that, while the Ca atoms are coplanar and define the (10$\bar{1}$4) plane, the oxygen triangles of the CO_3 groups are neither in nor parallel to the Ca-containing surface. Rather, the three oxygen atoms in the CO_3 groups are arranged in such a way that one lies in the plane and the other two are below and above, respectively (Figure 2B,C). Furthermore, whereas the above-plane O (O_a in Figure 2B) binds to a Ca (1 in Figure 2C) in the $-c$ direction (Ca$-$), the below-plane O (O_b in Figure 2B) is linked to a Ca (2 in Figure 2C) in the $+c$ direction (Ca+). If an etch pit forms after the removal of a CO_3 from the (10$\bar{1}$4) surface, the Ca$-$ will have an unsaturated bond pointing outward in the $+c$ direction. In contrast, the open bond on the Ca+ is inward in the $-c$ direction. Thus, if an aqueous carboxyl is to replace the missing CO_3 through surface binging, the negatively charged oxygen on the $-COO^-$ is able to descend onto the Ca$-$ freely but does not have easy access to the Ca+ (Figure 2B). Such a geometric arrangement makes it even more difficult for a larger ligand such as SUC (having two carboxyls) to bind to Ca+. We suggest the anisotropic appearance of the [010] steps results from the stereochemical differences surrounding the Ca+ and Ca$-$ atoms.

To sum up the experimental observations and the above discussion, we propose the following surface binding mechanism for SUC-calcite interactions (Figure 3):

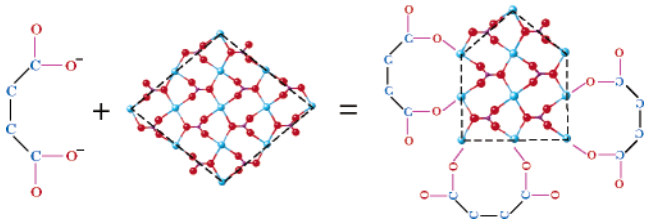

Figure 3. Graphical illustration of the proposed reaction mechanism showing the binding directions of SUC on calcite {10$\bar{1}$4} faces. Refer to Figure 1A for crystallographic orientations.

In light of earlier studies on ASP-calcite interactions,[4,7] the results reported here have several implications. First, they suggest that the amine group on ASP must be an active participant in surface binding. ASP differs from SUC only in the possession of the α-NH_2 group. If carboxyls are the sole functional groups involved in the surface binding, the edges of the etch pits developed in ASP and SUC solutions should have the same orientations. Yet, the steps seen in ASP (Figure 4) followed the [$\bar{4}$11] and [45$\bar{1}$], not the expected [42$\bar{1}$]. Second, they indicate that the involvement of the $-NH_2$ may be direction dependent as well. Although the [010] step did not manifest at low SUC concentrations (Table 1), and did not fully develop in ASP solutions at early stage of dissolution, it is well formed in both cases at high acid concentrations. Thus, if the α-amine group plays important roles for the development of the [$\bar{4}$11] and [45$\bar{1}$] pit edges, it does not seem to impact the development of [010] step. Last, as expected, the etch pits seen in SUC were highly symmetric, implying that chiral molecules are necessary to induce symmetry breaking around the *c*-glide plane of {10$\bar{1}$4} faces.

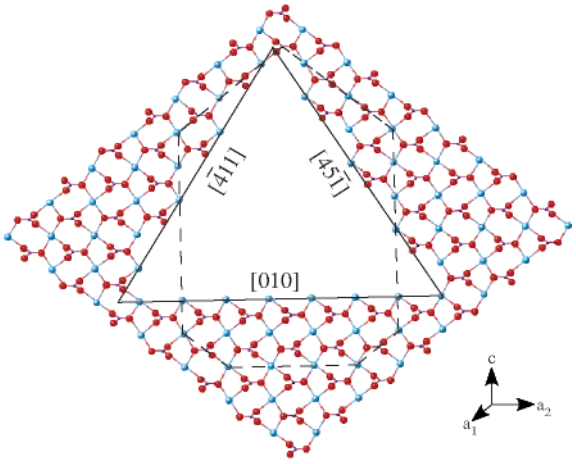

Figure 4. A comparison of the step directions developed in ASP (dash lines) and SUC (solid lines) on calcite {10$\bar{1}$4} faces.

Acknowledgment. This work was supported by the U.S. National Science Foundation (EAR, 0229634) and the National Natural Science Foundation of China (Joint Research Fund for Overseas Young Scholars, Grant 40428004). We are grateful for valuable comments and suggestions from two reviewers.

References

(1) (a) Inskeep, W. P.; Bloom, P. R. *Soil Sci. Soc. Am. J.* **1986**, *50*, 1167−1172. (b) Reddy, M. M.; Hoch, A. R. *J. Colloid Interface Sci.* **2001**, *235*, 365−370. (c) Wada, N.; Okazaki, M.; Tachikawa, S. *J. Colloid Interface Sci.* **2001**, *233*, 65−72. (d) Zuddas, P.; Pachana, K.; Faivre, D. *Chem. Geol.* **2003**, *201*, 91−101. (e) Perry, T. D., IV; Duchworth, O. W.; Kendall, T. A.; Martin, S. T.; Mitchell, R. *J. Am. Chem. Soc.* **2005**, *127*, 5744−5745.

(2) (a) Geffroy, C.; Goissy, A.; Persello, J.; Cabane, B. *J. Colloid Interface Sci.* **1999**, *211*, 45−53. (b) Lee, Y. J.; Reeder, R. J.; Wenskus, R. W.; Elzinga, E. J. *Geochim. Cosmochim. Acta* **2005**, *69*, 49−61.

(3) Mann, S. *Biomineralizaiton: Principles and Concepts in Bioinorganic Materials Chemistry*; Oxford University Press: New York, 2001.

(4) (a) Orme, C. A.; Noy, A.; Wierzbicki, A.; McBride, M. T.; Grantham, M.; Teng, H. H.; Dove, P. M.; DeYoreo, J. J. *Nature* **2001**, *411*, 775−778. (b) Teng, H. H.; Dove, P. M.; Orme, C. A.; De Yoreo, J. J. *Science* **1998**, *282*, 724−727.

(5) (a) Hazen, R. M.; Sholl, D. S. *Nat. Mater.* **2003**, *2*, 367−374. (b) Hazen, R. M.; Filley, T.; Goodfriend, G. *Proc. Nat. Acad. Sci. U.S.A.* **2001**, *98*, 5487−5490.

(6) (a) Berman, A.; Ahn, D. J.; Lio, A.; Salmeron, M.; Reichert, A.; Charych, D. *Science* **1995**, *269*, 515−518. (b) Söllner, C.; Burghammer, M.; Busch-Nentwich, E.; Berger, J.; Schwarz, H.; Riekel, C.; Nicolson, T. *Science* **2003**, *302*, 282−286.

(7) Teng, H. H.; Dove, P. M. *Am. Mineral.* **1997**, *82*, 878−887.

(8) (a) Agarwal. P.; Berglund, K. A. *Cryst. Growth Des.* **2003**, *3* (6), 941−946. (b) Agarwal, P.; Yu, Q.; Harant A.; Berglund; K. A. *Ind. Eng. Chem. Res.* **2003**, *42*, 2881−2884.

(9) Mann, S.; Didymus, J. M.; Sanderson, N. P.; Heywood, B. R.; Aso Samper, E. J. *J. Chem. Soc. Faraday Trans.* **1990**, *86* (10), 1873−1880.

(10) (a) Aizenberg, A. J.; Albeck, S.; Weiner, S.; Addadi, L. *J. Crystal Growth* **1994**, *142*, 156−164. (b) Aizenberg, A. J.; Black, G. M.; Whitesides, G. *J. Am. Chem. Soc.* **1999**, *121*, 4500−4509.

(11) (a) Stipp, S. L.; Eggleston, C. M.; Nielsen, B. S. *Geochim. Cosmochim. Acta* **1994**, *58*, 3023−3033. (b) Liang, Y.; Baer, D. R.; McCoy, J. M.; Amonette, J. E.; LaFemina, J. P. *Geochim. Cosmochim. Acta* **1996**, *60*, 4883−4887.

(12) Reeder, R. J. *Rev. Mineral.* **1983**, *11*, 1−47.

(13) (a) Titiloye, J. O.; Parker, S. C.; Mann, S. *J. Crystal Growth* **1993**, *131*, 533−545. (b) de Leeuw, N. H.; Parker, S. C.; Harding, J. H. *Phys. Rev. B: Condens. Matter Mater. Phys.* **1999**, *60*, 13792−13799.

(14) (a) Sangwal, K. *Etching of Crystals: Theory, Treatment, and Application*; Elsevier: Amsterdam, The Netherlands, 1987. (b) Rajam, S.; Mann, S. *J. Chem. Soc., Chem. Commun.* **1990**, 1789−1791.

(15) Mann, S. *Nature* **1988**, *332*, 119−124.

JA063167M